

## Article

# A Quasi-Nondestructive Evaluation Method for Physical-Mechanical Properties of Fragile Archaeological Wood with TMA: A Case Study of an 800-Year-Old Shipwreck

Mengruo Wu <sup>1</sup>, Xiangna Han <sup>1,\*</sup>, Zhenfang Qin <sup>1</sup>, Zhiguo Zhang <sup>2</sup>, Guanglan Xi <sup>1,2</sup> and Liuyang Han <sup>1,3,\*</sup>

- <sup>1</sup> Institute of Cultural Heritage and History of Science & Technology, University of Science and Technology Beijing, Beijing 100083, China; wumengruo@163.com (M.W.); 18435222442@163.com (Z.Q.); xiguanglan@126.com (G.X.)
- <sup>2</sup> National Center of Archaeology, Beijing 100020, China; zzwgws@126.com
- <sup>3</sup> Institute for Conservation of Cultural Heritage, University of Science & Technology Beijing, Beijing 100083, China
- \* Correspondence: jayna422@126.com (X.H.); hanliuyang@ustb.edu.cn (L.H.)

**Abstract:** Archaeological wood is a kind of ‘new material’ that has deteriorated due to long-term degradation. The existing wood science theory and evaluation methods are not fully applicable to archaeological wood. Moreover, current physical-mechanical evaluation methods are inadequate for fragile archaeological wood due to their insufficient accuracy and the large sample amount required, causing difficulties in many necessary physical-mechanical repeatability tests. In light of these limitations, the representative samples on Nanhai No. 1, a merchant shipwreck in the Song Dynasty, were selected as the research objects in this paper. The shipwreck is a typical waterlogged wooden artifact. A quasi-nondestructive physical-mechanical evaluation technique for archaeological wood was developed with the thermomechanical analyzer (TMA). This study used TMA to evaluate the bending strength of representative waterlogged archaeological samples of Nanhai No. 1 shipwreck and sound wood with the same species. Besides, the thermal linear expansion coefficients in the ambient temperature range were obtained. The sizes of the samples used in the tests were only 2 mm × 8 mm × 0.3 mm and 1 cm × 1 cm × 1 cm, respectively. Bending strength results of archaeological wood by the TMA method conformed to the tendency that the bending strength decreases with the increase of decay degree. In addition, the longitudinal linear expansion coefficients of archaeological wood reached 80%–115% of those in the transverse grain direction, which were about 10 times higher than those of the sound wood. The linear expansion coefficients of archaeological wood in three directions were similar. Based on the results of Fourier transform infrared analysis (FT-IR), the significant differences in the physical-mechanical properties of the archaeological wood and the sound wood were induced to be mainly ascribed to the decomposition and the loss of hemicellulose in the archaeological wood. The cell wall substrate could not stabilize the cellulose skeleton, which led to the instability of the tracheid structure of the archaeological wood. This study provided a proven quasi-nondestructive method for the preservation state evaluation of waterlogged archaeological wood (WAW) from the Nanhai I shipwreck and other similar waterlogged wooden relics.

**Keywords:** wooden artifacts; thermomechanical analysis; bending strength; thermal expansion



**Citation:** Wu, M.; Han, X.; Qin, Z.; Zhang, Z.; Xi, G.; Han, L. A Quasi-Nondestructive Evaluation Method for Physical-Mechanical Properties of Fragile Archaeological Wood with TMA: A Case Study of an 800-Year-Old Shipwreck. *Forests* **2022**, *13*, 38. <https://doi.org/10.3390/f13010038>

Academic Editors: Yoon Soo Kim and Adya P. Singh

Received: 1 December 2021

Accepted: 28 December 2021

Published: 1 January 2022

**Publisher’s Note:** MDPI stays neutral with regard to jurisdictional claims in published maps and institutional affiliations.



**Copyright:** © 2022 by the authors. Licensee MDPI, Basel, Switzerland. This article is an open access article distributed under the terms and conditions of the Creative Commons Attribution (CC BY) license (<https://creativecommons.org/licenses/by/4.0/>).

## 1. Introduction

The wooden cultural relics usually refer to shipwrecks, wooden production tools, wooden beds, wood carvings, coffins, and other artifacts left over from the social activities of humans. These relics contain rich historical information and are precious physical evidence for studying ancient science, technology, art, and culture. In recent years, massive waterlogged wooden artifacts have been excavated in China, such as the Nanhai No. 1

shipwreck and Xiaobaijiao I shipwreck [1]. Its overall protection and long-term safe and stable preservation are significant. According to the protection experience of the discovered marine shipwrecks, such as the Vasa shipwreck in Sweden [2] and the British Mary Rose shipwreck [3], the assessment of wood preservation is the premise for the scientific protection of these relics. Most archaeological wood has a high decay degree and a complex degradation mode caused by chemical, biological, and other factors [4]. Its cell wall structure and properties have seriously deteriorated, making it a “new” material different from sound/recent wood [5]. The heterogeneous degradation of the archaeological wood also increases the difficulty of sampling and testing. Thus, the existing wood theory is not suitable for this material.

Previous researchers have evaluated the preservation of waterlogged archaeological wood with many exploration efforts, among which mechanical properties have attracted great attention as an important evaluation index. Present, researches on the mechanical properties of waterlogged archaeological wood have mainly focused on the macro level. Most studies use a universal mechanical testing machine to obtain the compressive strength, bending strength, elastic modulus, and hardness along the grain [6,7]. Due to the limitation of micro-destructive and non-destructive sampling of wood, non-standard samples rather than national standard samples are often made to evaluate the mechanical properties of the discovered marine wooden artifacts. Although universal mechanical test machines can give the mechanical properties of the samples, most of them are destructive. Even if non-standard samples are adopted, required specimens remain large, consuming numerous archaeological woods. To avoid the destruction of cultural relics in the research process, scholars have tried various non-destructive or micro-destructive evaluation methods, such as the ultrasonic method [8], nano-indentation technique [1,9]. However, the uneven degradation of wooden artifacts, the limitation of sampling volume and sample size, and the application scope of testing instruments have greatly limited the application of common physical-mechanical evaluation techniques for modern wood to archaeological wood. The quasi-nondestructive physical-mechanical characterization methods are suitable for fragile archaeological wood in urgent need of development.

The thermo-mechanical properties tests can be divided into the thermomechanical analysis (TMA) and the dynamic mechanical analysis (DMA) tests. The TMA selected in this research can evaluate how the deformation of the material is functionally related to the temperature under the action of programmed temperature control and non-vibration load, thus accurately measuring the deformation quantity of the specimen under the action of heat and force. TMA has been used to characterize the thermomechanical properties of various kinds of materials in many studies. It has been proven to be a simple and effective method to measure the glass transition temperature [10], soften temperature [10,11], and viscosity [12]. There have been studies using the TMA method to measure the softening point and creep characteristics of modified wood [13–15]. Moreover, TMA is also very commonly used to study the thermal expansion of polymer [16,17], inorganic non-metallic [18], and composite materials [19,20]. The DMA method has also been used to study the thermal expansion coefficient, but it is more complex than the TMA method due to its frequency effect [21]. In measuring viscoelasticity and related storage modulus loss modulus, the DMA method is highly effective [22]. Previously, some scholars have obtained the storage modulus and loss modulus of waterlogged archaeological wood by DMA under vibration load using small samples [23,24]. However, there were no reports about thermal expansion coefficient or the mechanical properties testing of archaeological wood by TMA. Compared with DMA and general mechanical testing methods, the TMA has higher test accuracy and smaller static load [20], thus meeting the requirements of fragile wooden artifacts. The thermal expansion coefficient can be easily measured and the applicability of TMA being used for archaeological wood mechanical testing can be explored. The sample thickness required for TMA is at millimeter or even micron level, which belongs to a quasi-nondestructive method. Therefore, TMA technology is deemed suitable

for developing a set of quasi-nondestructive physical-mechanical evaluation methods for fragile wooden artifacts.

In this paper, *Pinus* sp., the main wood species of the Nanhai No. 1 shipwreck, was taken as the research object. TMA was applied to evaluate the bending strength and linear expansion coefficient of archaeological wood. The evaluation of decay degree, observation of anatomical structure, and chemical structure analysis were carried out to explain why the physical-mechanical properties of archaeological wood decreased. This research verified the feasibility of the physical-mechanical properties of archaeological wood by the TMA technology.

## 2. Materials and Methods

### 2.1. Materials

The Nanhai No. 1 shipwreck is a wooden shipwreck that sank into the sea during the Song Dynasty more than 800 years ago. The shipwreck with 41.8 m long, 11 m wide, and 4 m in height was found in the waters of Guangdong, China, in 1987 [25]. It is the oldest, largest, and most well-preserved ocean-going merchant ship found in the world so far, which can provide precious information for restoring the history of the Maritime Silk Road [26]. In 2007, the Nanhai No. 1 shipwreck was salvaged as a whole in the huge box, which is now exhibited and protected in the Maritime Silk Road Museum. Given the huge volume and complex structure of this shipwreck, it is urgent to verify the decay degree of hull wood scientifically to develop the appropriate conservation schedule. Therefore, representative samples collected from the end of the panel (named N3), from the inner part of the panel (named N2), and a sample from a hull component (named N1) were selected to carry out this research. Wood identification was according to our previous publication [27]. The wood pieces no less than 0.5 cm (longitudinal, L) × 0.5 cm (radial, R) × 0.5 cm (tangential, T) were cut off from the waterlogged archaeological wood. The longitudinal, radial, and tangential sections with a thickness of about 15 μm–20 μm were prepared by the sliding slicer (Leica M205C, Leica, Baden-Württemberg, Germany). The microscopic optical slices were prepared by dyeing, dehydration, transparency, and sealing according to our previous publication [28]. The microstructure characteristics of the wood were observed under an optical microscope (BX 50, Olympus, Tokyo, Japan). After referring to IAWA's list of wood identification characteristics for hardwood and compared with the wood specimens and slices officially named in the Wood Collection of Chinese Academy of Forestry (<http://bbg.criwi.org.cn>, 11 October 2021), the species of the waterlogged archaeological wood was determined. The sound wood of *Pinus* sp. (Longyan City, Fujian Province, 25° N, 115° E, 390 m a.s.l., 35 years old, 30 cm DBH) was selected as the reference sample, named R1.

The Basic Density (*BD*) and Maximum Water Content (*MWC*) of waterlogged archaeological wood were calculated according to Equations (1) and (2) respectively [29]. The mass of the waterlogged sample with the size of about 10 mm × 10 mm × 10 mm was measured by the analytical balance (JA2003, SUNNY HENGPING Instrument, Shanghai, China) and recorded as  $M_1$ . After being dried in an oven at  $103 \pm 2$  °C, the mass of the sample was recorded as  $M_0$ . The drainage method was used to measure the waterlogged volume  $V_1$ . On the analytical balance, the sample was completely immersed in pure water without touching the bottom and wall of the beaker. According to Archimedes' principle, the volume of the wood sample (cm<sup>3</sup>) equals the increased mass (g) in value of the pure water.

$$BD = \frac{M_0}{V_1} \quad (1)$$

$$MWC = \frac{M_1 - M_0}{M_0} \times 100\% \quad (2)$$

## 2.2. Chemical Analysis

The relative contents of the alcohol-benzene extractives, lignin, and ash in the waterlogged archaeological wood can be obtained by wet chemical analysis (WCA), and the holocellulose content was calculated as 100% minus the contents of all the components measured above. Compared with the results of sound wood, the decay degree of the waterlogged archaeological wood can be evaluated. Refer to GB/T 2677.8-1994 [30] and GB/T 2677.3-1993 [31] for the test methods of this part.

Fourier transform infrared spectroscopy (FT-IR) was used to characterize the chemical structure of wood, then the differences in characteristic functional groups between archaeological wood and sound wood were compared by semi-quantitative analysis. The absolute dry mass ratio of wood sample to potassium bromide powder was 1:100. Study samples were tested by Nicolet™ iS™5 Fourier transform infrared spectrometer (Thermo Scientific, Waltham, MA, USA) with 32 scanning times and 4.000 resolution. The test data was processed by EZ OMNIC 7.3 (Thermo Scientific, Waltham, MA, USA) and Origin 2019b (OriginLab, Northampton, MA, USA).

## 2.3. Bending Strength Measurements by TMA

The thermomechanical analyzer (TMA) used in this work is HITACHI TMA7100 (HITACHI analyzer, Tokyo, Japan). It has a load range of  $\pm 5.8$  N, a load resolution of  $9.8 \mu\text{N}$ , a displacement resolution of  $0.01 \mu\text{m}$ , a scope of temperature test of  $-60$  °C to  $450$  °C, and a temperature resolution of  $10^{-8}$  °C. The structure and schematic diagram of TMA are shown in Figure 1.

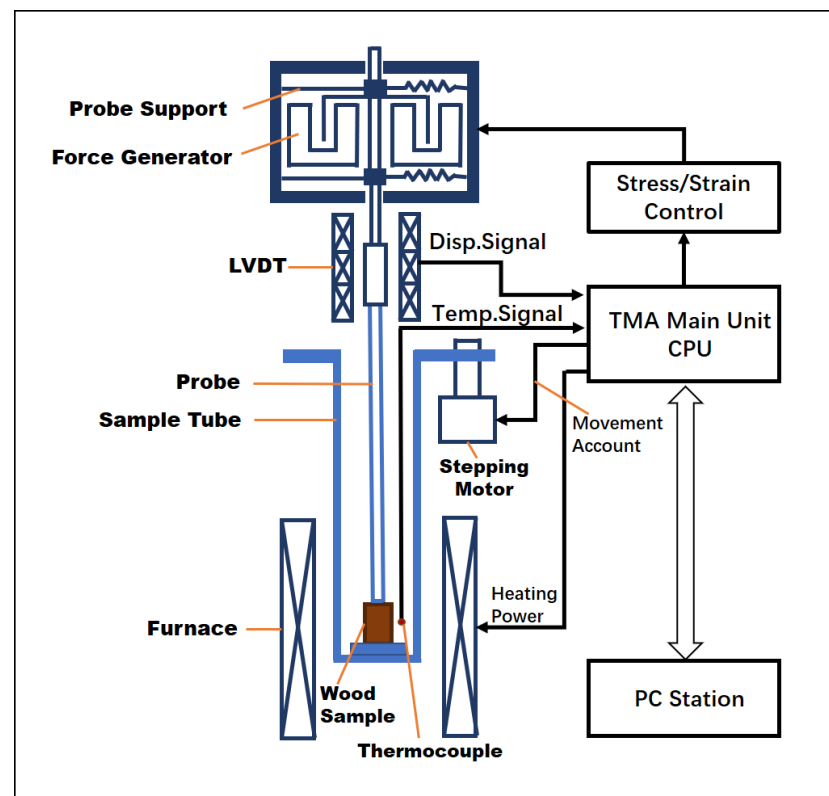


**Figure 1.** Schematic diagram of TMA (modified following an original drawing provided by HITACHI TMA7100 operation manual).

The specimen preparation processes of bending strength were as follows: Leica 2010R slicer was used to prepare waterlogged archaeological wood slices of about  $20 \text{ mm} \times 20 \text{ mm} \times 0.3 \text{ mm}$  ( $L \times R \times T$ ), and the specimens of TMA bending strength of about  $10 \text{ mm} \times 2 \text{ mm}$  ( $L \times R$ ) were manually cut after drying. In the bending strength test, quartz bending probe and

supporting components were used, with a span  $L = 5$  mm as shown in Figure 2. The test was carried out at room temperature with an initial load of 0.1 mN and a loading speed of 5 mN/min until the specimen was broken (Figure 3b). The real-time displacement  $D$  curve and load  $F$  curve of the probe were obtained (Figure 3c). The width  $b$  and the thickness  $d$  of the sample were measured by VHX-6000 ultra-depth three-dimensional microscope (KEYENCE, Ōsaka, Japan) with an accuracy of 0.01 mm. The bending strength  $\sigma$  and the failure strain  $\varepsilon$  were calculated by Equations (3) and (4) [32], with at least 30 samples in each group. The average value of the data in the 95% confidence interval was taken as the result of the bending strength of the sample, and ANOVA analysis of variance was used to analyze the bending strength data.

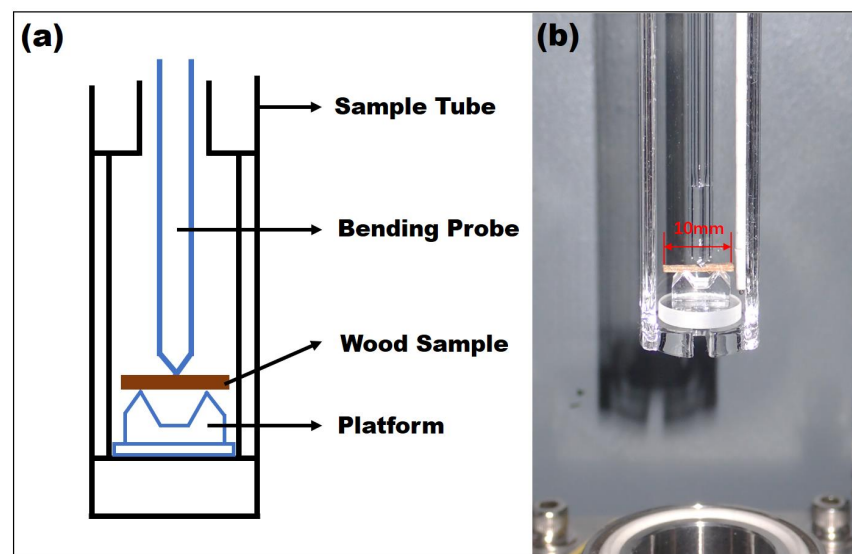


**Figure 2.** Mechanical properties of archaeological wood tested with TMA: (a) schematic diagram of bending test components; (b) image of bending test.

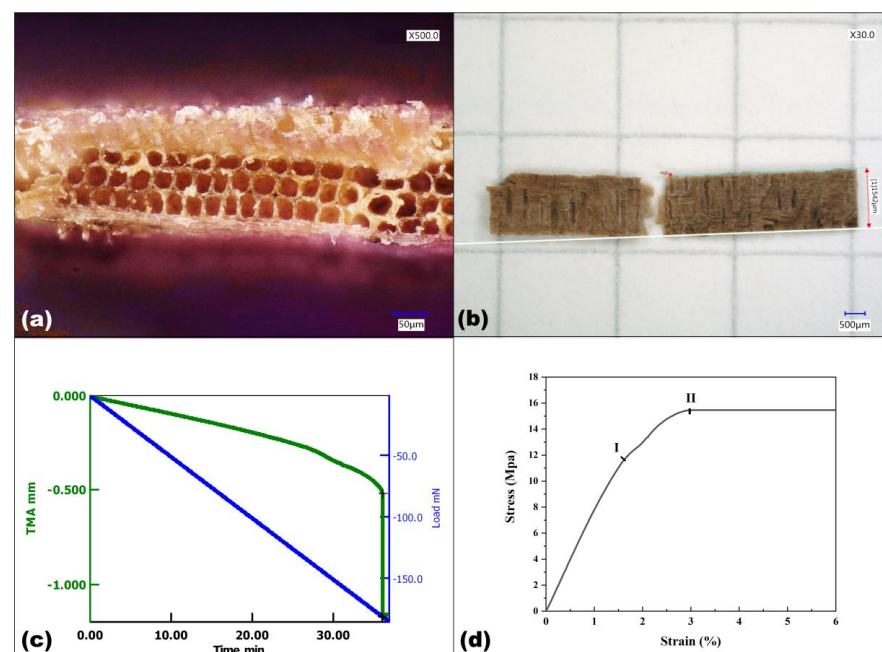


**Figure 3.** Bending test of archaeological wood with TMA (taking a sample of N1 as an example): (a) Failure morphology; (b) Failure position; (c) Load-time and displacement-time test curves. Negative values represented the direction of load and displacement was downward; (d) Stress-strain curve.

In the stress-strain curve (Figure 3d), it could be recognized that point 0–I was the elastic deformation range, I–II was the plastic deformation yield stage, and the bending failure point was at point II.

$$\sigma_f = \frac{3FL}{2bd^2} \quad (3)$$

$$\varepsilon_f = \frac{6Dd}{L^2} \quad (4)$$

#### 2.4. Coefficients of Thermal Linear Expansion Measurements by TMA

The dimensional stability under environmental fluctuation is an important physical property that determines the structural safety of wooden artifacts, and the linear expansion coefficient can be used as an evaluation index. The temperature ranging from  $-10\text{ }^{\circ}\text{C}$  to  $50\text{ }^{\circ}\text{C}$  was designed to simulate the temperature change during the storage of wooden artifacts in this study. The samples with a size of less than  $1\text{ cm} \times 1\text{ cm} \times 1\text{ cm}$  were selected and dried by supercritical fluid drying technology [33], then the samples were cut to make their surfaces smooth. The quartz compression probe and platform used in the test are shown in Figure 4. The initial length of the sample was recorded as  $l_0$ . The test temperature range was  $-40\text{ }^{\circ}\text{C}$  to  $70\text{ }^{\circ}\text{C}$ , and the heating rate was  $5\text{ }^{\circ}\text{C}/\text{min}$ . The average linear expansion coefficient  $\alpha$  in the temperature range ( $T_1, T_2$ ) was calculated by Equation (5), where  $l_{T_1}$  and  $l_{T_2}$  were the sample lengths corresponding to  $T_1$  and  $T_2$ . The linear expansion coefficients in the longitudinal, radial, and tangential directions of wood samples were denoted as  $\alpha_l$ ,  $\alpha_r$ , and  $\alpha_t$ , respectively. Each group of samples was tested three times and the average value was taken.

$$\alpha = \frac{l_{T_2} - l_{T_1}}{l_0(T_2 - T_1)} \quad (5)$$

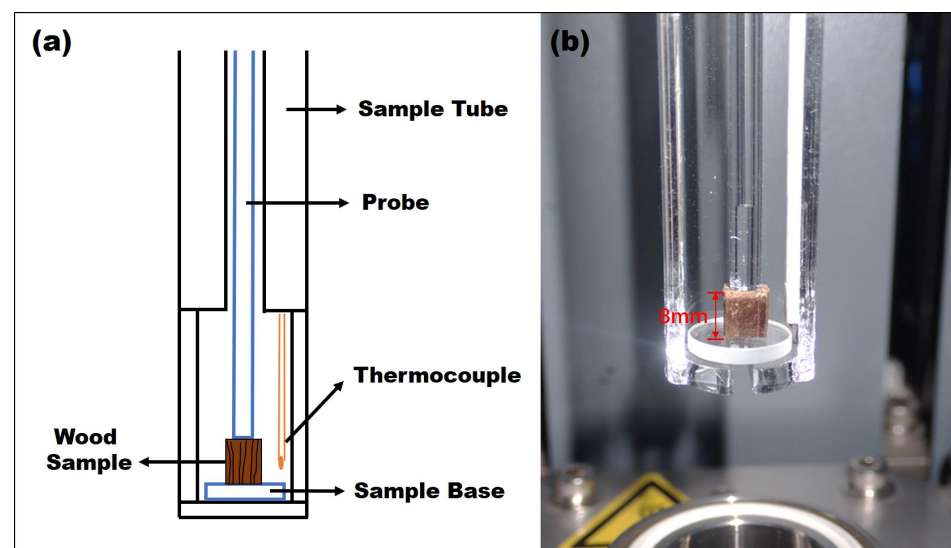


**Figure 4.** Linear expansion coefficient of archaeological wood tested with TMA: (a) linear expansion test components; (b) image of linear expansion test.

### 3. Results

#### 3.1. Basic Information and Decay Degree of Archaeological Wood

Figure 5 shows the morphological structures of waterlogged archaeological wood samples N1–N3, which were identified as *Pinus* spp. As can be seen from the figure, the pine had apparent growth circles; while the transition from early-wood to late-wood changes rapidly. Tracheid in cross-sections were mostly long-sided, square, and polygonal. Tracheid pitting in radial walls uniseriate, with the presence of ray tracheid. The cell walls of ray tracheid were dentate, with prominent dentations; by contrast, the end-walls of ray

parenchyma were smooth. Cross-field pitting was “window-like”, and mostly had 1–2 per cross field. The ray height was 2–12 cells. Axial and radial resin ducts presented, with 8–10 thin-walled epithelial cells (Figure 5). Tracheids of late-wood of N1, N2, and N3 had a certain degree of deformation. Some cell walls are separated from the intercellular layer (Figure 5a,d,g), indicating that the waterlogged archaeological wood selected in this study had deteriorated to a certain extent.

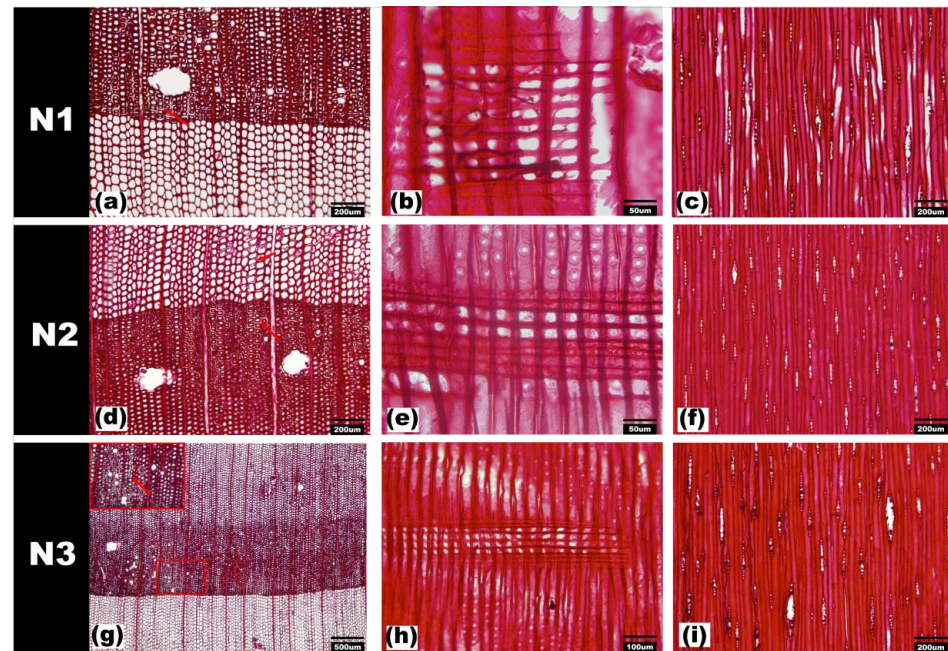


**Figure 5.** Anatomical structure of archaeological wood under an optical microscope. The cross-section, radial section, and tangential section of N1 were shown in (a–c), N2 in (d–f), and N3 in (g–i). It could be seen in (a,d,g) that the cell wall of some cells was separated from the intercellular layer, as indicated by the arrow.

Maximum Water Content (MWC) and Basic Density (BD) are important indicators in evaluating the preservation status of waterlogged archaeological wood. Generally, when the MWC of a waterlogged archaeological wood exceeds 400%, its decay degree is deemed as severely decayed. The value of MWC between 185% and 400% indicates moderately decayed and below 185% slightly decayed [34].

The results of MWC and BD showed that (Figure 6), N1 had the smallest MWC, which was 345.27%, followed by N2, which was 452.03%, and N3 had the largest MWC, which was 488.61%. The BD decreased with the increase of MWC. The BD values of N1–N3 were  $0.242 \text{ g}\cdot\text{cm}^{-3}$ ,  $0.194 \text{ g}\cdot\text{cm}^{-3}$ ,  $0.187 \text{ g}\cdot\text{cm}^{-3}$ , respectively. According to the above results, N1 was moderately decayed with the lowest water content, both N2 and N3 were severely decayed.

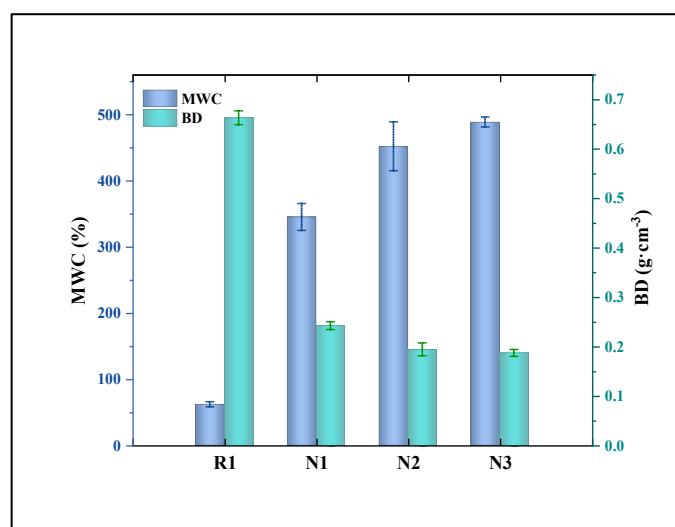


**Figure 6.** MWC and BD of the archaeological wood.

### 3.2. Chemical Analyses

The results of the wet chemical test (Figure 7) showed that the chemical composition of the archaeological wood changed compared with the sound wood. The alcohol-benzene extractives content of archaeological wood decreased to 60%~70% of the sound wood with rising degradation degree, which might be due to the dissolution of soluble substances in wood cells during the long-time immersion. The average relative content of holocellulose in the *Pinus* sp. archaeological wood was 20.45%, about 33% that of the sound wood. Due to the significant decrease in the relative content of holocellulose, the average relative content of lignin in the archaeological wood increased to 68.34%, about 2.6 times that of the sound wood. In addition, it was found that the relative contents of the holocellulose slightly decreased with the increase of the decay degree of the waterlogged archaeological wood, while the relative content of lignin increased with the increase of the decay degree. As for the N3 sample, its holocellulose content was only 19.07%, while its lignin content was up to 69.32%. Besides, the ash relative contents of archaeological wood were 3.59%, 3.18%, and 5.05% for N1, N2, and N3 while only 0.17% for sound wood, which had significantly increased to about 20~30 times.

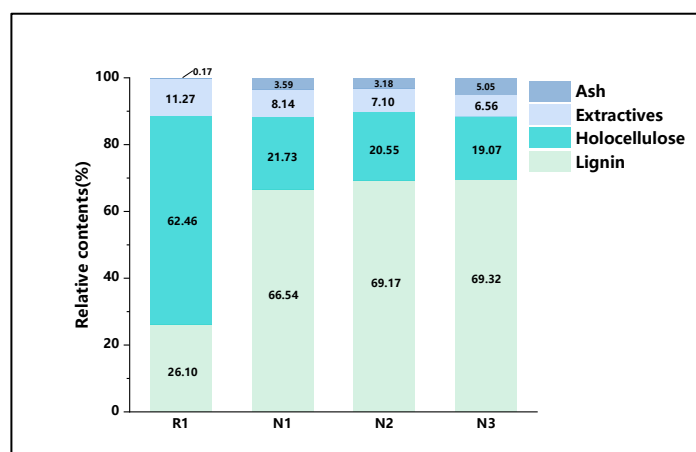


**Figure 7.** Relative contents of lignin, holocellulose, alcohol-benzene extractives, and ash of the archaeological wood.

The Fourier transform infrared analysis (FT-IR) results of the archaeological wood samples and their reference samples are shown in Figure 8a. In the spectra of the archaeological wood samples, the characteristic band peaked at  $1730\text{ cm}^{-1}$  ascribed to the C=O

stretching of hemicellulose, and the band at  $1318\text{ cm}^{-1}$  belonging to the  $\text{CH}_2$  out-of-plane vibration of cellulose [35] shifted obviously. Besides, the peak intensity decreased with the increase of decay degree. The intensity ratios of the absorption peak of the lignin functional group to the peak of C-H bending vibration of holocellulose at  $1370\text{ cm}^{-1}$  were calculated according to the infrared spectrum (Figure 8b). As holocellulose is more prone to degradation than lignin in an immersion environment [36], the difference in the degree of chemical structural change in the three kinds of archaeological wood could be characterized by the peak intensity ratio [1]. A larger ratio means greater loss of holocellulose and heavier decay of wood. Results showed that the intensity ratio of the absorption peaks belonging to lignin had increased significantly with the increase of the decay degree, such as the extensional vibration of the benzene ring at  $1509\text{ cm}^{-1}$  [37], C-C and C-O at  $1223\text{ cm}^{-1}$ , and G-type lignin C=O at  $1265\text{ cm}^{-1}$  [35].

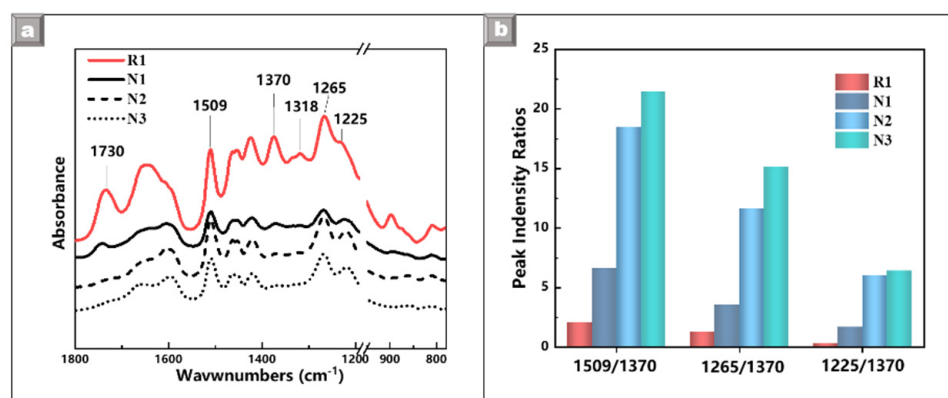


**Figure 8.** FT-IR spectra (a) and characteristic absorption peak intensity ratio (b) of the archaeological wood.

The analysis of chemical composition and structure showed that polysaccharides were firstly decomposed in a large amount during the degradation process. Notably, hemicellulose had the greatest structural change, and its content decreased significantly. Cellulose was also decomposed to some extent. Compared with hemicellulose and cellulose, lignin is more stable and only slightly decomposed, so its relative content in the archaeological wood increased. Due to the preferential decomposition [38] of polysaccharides by microorganisms such as erosion bacteria and brown-rot fungi, the increase of lignin content can be commonly seen during the degradation of the waterlogged archaeological wood. A significant increase in ash content is a common scene in the archaeological wood, which is presumed to mainly come from inorganic salt deposits in archaeological wood samples or mineralization caused by microbiological decomposition [7,39]. The changes in chemical composition and chemical structure are likely to lead to the decrease of mechanical strength and changes in the physical properties of the archaeological wood.

### 3.3. Bending Strength

The archaeological wood samples involved in the study are selected from the shipboard, whose stress patterns are mainly of the upper surface bending and the lower surface stretching, which means that the bending strength is the main index to characterize its mechanical properties. However, sometimes the bending test could not be performed since it was difficult to obtain clear specimens of sufficient length [40]. This study obtained the bending strength of three groups of archaeological wood samples by the quasi-nondestructive thermomechanical analyzer (TMA), aiming to clarify the factors affecting the mechanical properties of archaeological wood.

Data of mechanical property with a confidence level above 0.95 were selected as valid data in this research, as shown in Figure 9a. The average bending strength values of the samples N1–N3 were calculated to be  $5.990 \pm 4.156$  Mpa,  $4.583 \pm 2.458$  Mpa, and  $4.097 \pm 1.844$  Mpa, respectively; while that value of the sound wood was  $38.982 \pm 22.760$  Mpa

(Figure 7). After analyzing the bending strengths of the waterlogged archaeological wood and the sound wood with ANOVA, it was found that the means were significantly different at the 0.05 level. The comparison of the means showed that the mechanical strength values of the three groups of archaeological wood were at the same level, lower than that of the sound wood. Compared with the sound wood, the bending strengths of the three groups of archaeological wood decreased by 84.6%, 88.24%, and 89.49%, respectively.

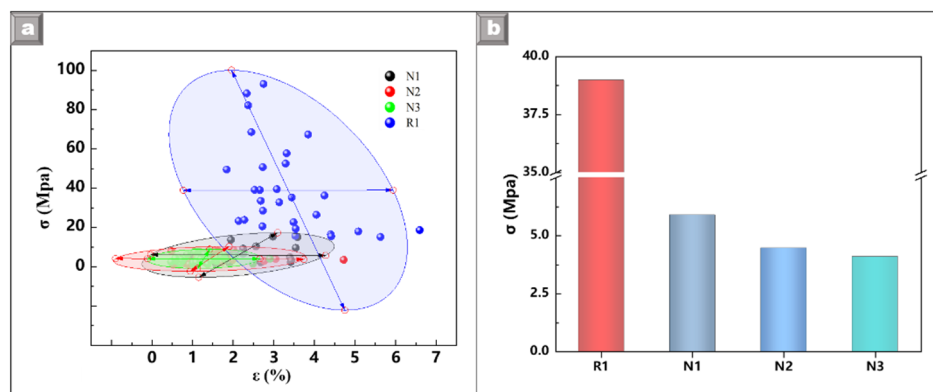


**Figure 9.** (a) Bending strength–failure strain and 95% confidence interval of archaeological wood; (b) Mean bending strengths of each group of samples.

Hoffman et al. have conducted a long-term bending test on the ship plank from Vasa [41]. The visible bending deformation of the archaeological wood under constant load has been observed although no absolute value of the flexural strength obtained. Some scholars have used a universal testing machine to test the mechanical properties of degraded wood immersed in seawater for half to five years. The results show that the bending strength of English oak wood was reduced from 114 Mpa to 99.7~49 Mpa (about 12%~58%) [42–44]; that of the spruce and Pinus immersed in freshwater for 70~140 years decreased by 40% [45]. According to the above references, the bending deformation of archaeological wood is much more severe than that of healthy wood, and the bending strength decreases as the degree of degradation increases. This work also proved this conclusion, and the result obtained in this study is more persuasive given the high degree of degradation. Among the three groups of archaeological wood, means comparison showed that the bending strength of moderately decayed N1 was different from that of severely decayed N2 and N3. The test results of mechanical properties were consistent with those of MWC. With the increase of MWC, the bending strengths of the archaeological wood samples decreased in turn, and the bending strengths of the archaeological woods with the same decay degree were similar, which meant that the mechanical properties of the archaeological woods decreased with the increase of their decay degree. For the failure strains, the values of the archaeological woods were 67.71%, 45.91%, and 38.27% of the reference samples, respectively (Figure 9a). Consistent with the results of the bending strength, the failure strains of the archaeological woods with different decay degrees (N1, N2, and N3) were significantly different. The failure strain decreased with the increase of MWC, indicating that the bending toughness of the archaeological wood also decreased with the increase of the decay degree.

### 3.4. Coefficient of Thermal Linear Expansion

The test results of the thermal linear expansion coefficients of the archaeological wood samples in three anatomical directions were different from those of the sound wood in the range of  $-10$  °C to  $50$  °C. Figure 10a–c showed the thermal linear expansion coefficients of the archaeological wood samples and the sound wood sample in tangential, radial, and longitudinal directions, respectively. The tangential and radial thermal linear expansion coefficients ( $\alpha_t$ ,  $\alpha_r$ ) of archaeological wood were not significantly different from those of the

sound wood and decreased slightly with the increase of decay degree. However, the longitudinal thermal linear expansion coefficient  $\alpha_l$  of archaeological wood was significantly different from that of the sound wood, rising by about 10 times.

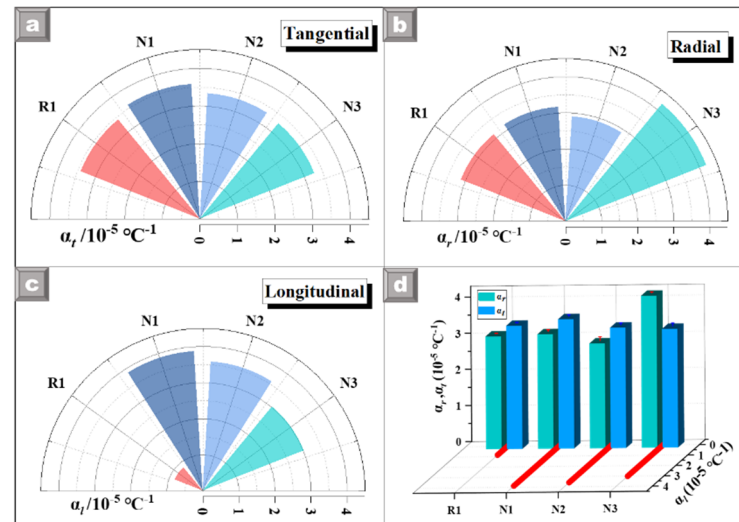


**Figure 10.** Results of Thermal linear expansion test of the archaeological wood. (a) Thermal linear expansion coefficient along the tangential direction. (b) Thermal linear expansion coefficient along the radial direction. (c) Thermal linear expansion coefficient along the longitudinal direction. (d) Comparison of expansion coefficients along and across the grain direction.

In general, the linear expansion coefficient along the grain direction ( $\alpha_l$ ) of sound wood is close to zero, only about 10% of that in the transverse grain direction. The radial linear expansion coefficient is smaller than that in the tangential direction [46–48]. The tendency of linear expansion of the three groups of archaeological wood samples in three directions was different from that of the sound wood. In detail, the  $\alpha_l$  of the archaeological wood was much larger. The linear expansion coefficients along the grain direction of samples N1 and N2 were about 115% and 82% of those along the transverse grain direction, respectively, 8–11.5 times that of the sound wood. The radial linear expansion coefficients of N1 and N2 were smaller than those in the tangential direction. However, the radial linear expansion coefficient of the N3 sample with the highest decay degree was slightly larger than that in the tangential direction.

#### 4. Discussion

Mechanical properties and dimensional stability are vital in evaluating the preservation status of wooden artifacts. For large-scale waterlogged wooden artifacts such as shipwrecks, the bending performance and dimensional stability in all directions determine whether the artifacts can remain stable for a long time. This explained why this research focuses on the bending strength and the linear expansion coefficients. Since the existing physical-mechanical evaluation methods cannot meet the specific needs of fragile wooden artifacts for testing instruments and methods of sample quantity and accuracy, this study developed an effective quasi-nondestructive characterization method of physical-mechanical properties based on the TMA technology.

In terms of mechanical properties, TMA provided a quasi-nondestructive test method that can effectively avoid excessive use of wood during the research process, with intuitive and reliable bending strength data obtained. Compared with the sound wood R1, the bending strengths of the three groups of archaeological wood have decreased by more than 80%. The results of three groups of archaeological wood samples with different decay degrees indicated that the bending strength decreased as the decay degree increased. Besides, the failure strain experienced the same trend, meaning that the brittleness of

archaeological wood gradually increased during degradation. Combined with the results of wet chemical analysis and FT-IR, it could be determined that the decrease of mechanical properties was related to the changes in chemical composition and chemical structure of wood cell walls. In general, hemicellulose in the wood cell walls was firstly decayed, followed by cellulose, while lignin was relatively stable [49]. With increasing decay degree, the relative content of lignin in the archaeological wood would gradually increase, and the relative content of polysaccharides mainly composed of hemicellulose decreases, which was significantly different from the chemical components of the sound wood. Some studies reported that when hemicellulose in sound wood was partially removed, the elastic modulus in the compression process could be reduced by more than 20%. In the nanoindentation experiment, elastic modulus and the hardness value were also reduced by more than 20% [9]. Matrix substances such as hemicellulose in the cell wall have a stabilizing and cross-linking effect on the long-chain cellulose skeleton structure [36]. Due to the great loss of hemicellulose in archaeological wood, the cellulose originally tightly wrapped in was more likely to bend or break [50]. This micro-level structural change led to a significant decrease in the macroscopic bending strength of wood.

On the other hand, the difference in longitudinal linear expansion tendency between the archaeological wood and the sound wood was found during the TMA linear expansion test. The longitudinal linear expansion coefficient of the archaeological wood was at least ten times higher than that of the sound wood. The linear expansion coefficient ( $\alpha_l$ ) along the grain direction of the sound wood was only about 10% that in the transverse grain direction, while the linear expansion rate along the grain direction of the archaeological wood reached 80% to 115% of that in the transverse grain direction. The tangential and longitudinal linear expansion coefficients of three groups of archaeological wood seemed to decrease slightly with the increase of decay degree. However, there was no obvious correlation between linear expansion coefficient and decay degree in general. The variation in the coefficient of linear expansion of ancient wood differs from that of sound wood, which may be explained by the decomposition of hemicellulose in archaeological wood [51,52]. Studies have shown that the longitudinal mechanical behavior of wood was mainly determined by cellulose [53]. Based on this, it was speculated that the significant increase in  $\alpha_l$  was caused by the large-scale decomposition of hemicellulose bound with cellulose. The cellulose absorbed a large amount of energy during heating, and the molecular spacing increased with the decrease of the binding force of the matrix substance, which made the linear expansion of the tracheid in the longitudinal direction easier [54,55]. In addition, the changes in the structure and the composition also affected the size change behavior in radial and tangential directions. Further study is required to find out why the linear expansion tendency of the archaeological wood is different from that of the sound wood.

## 5. Conclusions

Using the TMA method, this work evaluated the bending strength and thermal linear expansion coefficient of the fragile archaeological woods taken from the Nanhai No. 1 shipwreck. The bending strength values of moderately and severely decayed waterlogged archaeological wood were significantly lower than those of the sound wood. With the increase of decay degree, the mechanical properties decreased. The coefficients of linear expansion of the archaeological wood samples were significantly different from those of the sound wood. The effect of this abnormal linear expansion on the overall dimensional stability of the artifact may be noted when conserving waterlogged wooden artifacts.

Moreover, the TMA is proved to be an effective quasi-nondestructive method to evaluate the physical-mechanical properties of archaeological wood, which was useful for the evaluation of the state of preservation and the extent of deterioration. Research aiming to clarify the relationship between the measured physical-mechanical behaviors and other properties of archaeological wood will be continued, which will provide new methods with TMA for scientific cognitive research of archaeological wood and basic data for further protection of fragile wooden artifacts.

**Author Contributions:** Conceptualization, L.H. and X.H.; methodology, L.H.; software, M.W.; validation, X.H., L.H. and Z.Z.; formal analysis, L.H.; investigation, X.H., L.H. and Z.Q.; resources, Z.Z. and G.X.; data curation, X.H. and L.H.; writing—original draft preparation, M.W. and L.H.; writing—review and editing, M.W., X.H. and L.H.; visualization, M.W., X.H. and Z.Q.; supervision, X.H. and L.H.; project administration, X.H., Z.Z., G.X. and L.H.; funding acquisition, X.H. and L.H. All authors have read and agreed to the published version of the manuscript.

**Funding:** This research was funded by the National Key R&D Program of China, grant number 2020YFC1521801 and 2020YFC1521804.

**Institutional Review Board Statement:** Not applicable.

**Informed Consent Statement:** Not applicable.

**Data Availability Statement:** The data presented in this study are available on request from the corresponding author.

**Acknowledgments:** The authors would like to thank Yafang Yin, Xiaomei Jiang and Yonggang Zhang from Research Institute of Wood Industry, Chinese Academy of Forestry for the wood identification supports.

**Conflicts of Interest:** The authors declare no conflict of interest.

## References

- Han, L.; Tian, X.; Keplinger, T.; Zhou, H.; Li, R.; Svedström, K.; Burgert, I.; Yin, Y.; Guo, J. Even Visually Intact Cell Walls in Waterlogged Archaeological Wood Are Chemically Deteriorated and Mechanically Fragile: A Case of a 170 year-old Shipwreck. *Molecules* **2020**, *25*, 1113. [\[CrossRef\]](#)
- Hocker, E.; Almkvist, G.; Sahlstedt, M. The Vasa experience with polyethylene glycol: A conservator's perspective. *J. Cult. Herit.* **2012**, *13*, S175–S182. [\[CrossRef\]](#)
- Sandström, M.; Jalilehvand, F.; Damain, E.; Fors, Y.; Gelius, U.; Jones, M.; Salomé, M. Sulfur accumulation in the timbers of King Henry VIII's warship Mary Rose: A pathway in the sulfur cycle of conservation concern. *Proc. Natl. Acad. Sci. USA* **2005**, *102*, 14165–14170. [\[CrossRef\]](#)
- Walsh-Korbs, Z.; Averous, L. Recent developments in the conservation of materials properties of historical wood. *Prog. Mater. Sci.* **2019**, *102*, 167–221. [\[CrossRef\]](#)
- Blanchette, R. A review of microbial deterioration found in archaeological wood from different environments. *Int. Biodeterior. Biodegrad.* **2000**, *46*, 189–204. [\[CrossRef\]](#)
- Liu, L.; Zhang, L.; Zhang, B.; Hu, Y. A comparative study of reinforcement materials for waterlogged wood relics in laboratory. *J. Cult. Herit.* **2019**, *36*, 94–102. [\[CrossRef\]](#)
- Mauro, B.; Nicola, M. The wooden foundations of Rialto Bridge (Ponte di Rialto) in Venice: Technological characterisation and dating. *J. Cult. Herit.* **2019**, *36*, 85–93.
- Liu, Y.; Li, Z.; Zhang, X.; Teng, Q.; Yao, Z.; Hou, T.; Kitamori, A.; Lyu, H.; Que, Z. Application of Ultrasonic Nondestructive Testing Technology in Ancient Building Testing: Taking the lintel of the main hall of the Ancestral Temple of Shaolin Temple as an example. *Indust. Constr.* **2021**, *51*, 37–43.
- Konnerth, J.; Eiser, M.; Jäger, A.; Bader, T.K.; Hofstetter, K.; Follrich, J.; Ters, T.; Hansmann, C.; Wimmer, R. Macro- and micro-mechanical properties of red oak wood (*Quercus rubra* L.) treated with hemicellulases. *Holzforschung* **2010**, *64*, 447–453. [\[CrossRef\]](#)
- Qi, L.; Ma, Z.; Liang, J.; Xiao, Z.; Dong, M.; Zhang, J.; Guo, Z.; Fan, J.; Ding, T.; Liu, C. Thermomechanical investigation on the effect of nitroguanidine on the thermal expansion coefficient and glass transition temperature of double-base gun propellant. *J. Mater. Res. Technol.* **2019**, *8*, 4264–4272. [\[CrossRef\]](#)
- Stepanov, V.; Patel, R.B.; Mudryy, R.; Qiu, H. Investigation of Nitramine-Based Amorphous Energetics. *Propellants Explos. Pyrotech.* **2016**, *41*, 142–147. [\[CrossRef\]](#)
- Košťál, P.; Hofírek, T.; Málek, J. Viscosity measurement by thermomechanical analyzer. *J. Non-Crystall. Solids* **2018**, *480*, 118–122. [\[CrossRef\]](#)
- Mohammadi-Rovshandeh, J. Plasticization of poplar wood by benzylation and acetylation. *Iran. J. Offence Technol.* **2003**, *27*, 353–358.
- Sereshti, H.; Mohammadi-Rovshandeh, J. Chemical modification of beech wood. *Iran. Polymer J.* **2003**, *12*, 15–20.
- George, B.; Simon, C.; Properzi, M.; Pizzi, A.; Elbez, G. Comparative creep characteristics of structural glulam wood adhesives. *Holz Roh-Werkst.* **2003**, *61*, 79–80. [\[CrossRef\]](#)
- Saba, N.; Jawaid, M. A review on thermomechanical properties of polymers and fibers reinforced polymer composites. *J. Ind. Eng. Chem.* **2018**, *67*, 1–11. [\[CrossRef\]](#)
- Yang, H.-S.; Wolcott, M.; Kim, H.-S. Thermal properties of lignocellulosic filler-thermoplastic polymer bio-composites. *J. Therm. Anal. Calorim.* **2005**, *82*, 157–160. [\[CrossRef\]](#)

18. Wastiels, J.; Wu, X.; Faignet, S.; Patfoort, G. Mineral polymer based on fly ash. *J. Resour. Manag. Technol.* **1994**, *22*, 135–141.
19. Qi, L.; Zhang, S.-L.; Yuan, H.; Ma, Z.-L.; Xiao, Z.-L. A novel modification method for the dynamic mechanical test using thermomechanical analyzer for composite multi-layered energetic materials. *Def. Technol.* **2021**, *in press*. [[CrossRef](#)]
20. Liang, T.; Qi, L.; Ma, Z.; Xiao, Z.; Wang, Y.; Liu, H.; Zhang, J.; Guo, Z.; Liu, C.; Xie, W.; et al. Experimental study on thermal expansion coefficient of composite multi-layered flaky gun propellants. *Compos. Part B Eng.* **2019**, *166*, 428–435. [[CrossRef](#)]
21. Hong, G.; Wang, W.-Q.; Sun, L.; Han, J.-M.; Sasaki, K. The Dynamic Viscoelasticity of Dental Soft Polymer Material Containing Citrate Ester-Based Plasticizers. *Materials* **2020**, *13*, 5078. [[CrossRef](#)]
22. Le, V.D.; Caliez, M.; Gratton, M.; Frachon, A.; Picart, D. Mechanical characterisation of a viscous-elastic plastic material, sensitive to hydrostatic pressure and temperature. *Environ. Probl. Coastal Reg. VII* **2006**, *85*, 212–223. [[CrossRef](#)]
23. Pizzo, B.; Pecoraro, E.; Lazzeri, S. Dynamic mechanical analysis (DMA) of waterlogged archaeological wood at room temperature. *Holzforschung* **2018**, *72*, 421–431. [[CrossRef](#)]
24. Pecoraro, E.; Pizzo, B.; Salvini, A.; Macchioni, N. Dynamic mechanical analysis (DMA) at room temperature of archaeological wood treated with various consolidants. *Holzforschung* **2019**, *73*, 757–772. [[CrossRef](#)]
25. Wu, J.C.; Zhang, Y.Q. The overall salvage of the Nanhai No. 1" ancient sunken ship. *Navig. China* **2008**, *31*, 6.
26. Sun, J.; Liu, C.J. *The Archaeological Report of the Nanhai No. 1 Sunken Ship, II: Excavations from 2014 to 2015*; Cultural Relics Publishing House: Beijing, China, 2017.
27. Han, L.; Tian, X.; Zhou, H.; Yin, Y.; Guo, J. The Influences of the Anatomical Structure and Deterioration State of Wood from a Qing Dynasty Shipwreck on Wood Color after the Consolidation Treatment. *J. Southwest For. Univ.* **2020**, *40*, 1–7.
28. Dong, M.-Y.; Lu, Y.; Jiang, X.-M.; Wang, W.-B.; Zhou, Y.-C.; Zhao, G.-J.; Zhou, H.-B.; Yin, Y.-F. AMS 14C dating and wood identification in ancient timber structures in Shanxi Province, China. *J. Archaeol. Sci. Rep.* **2017**, *13*, 361–371. [[CrossRef](#)]
29. Macchioni, N.; Capretti, C.; Sozzi, L.; Pizzo, B. Grading the decay of waterlogged archaeological wood according to anatomical characterisation. The case of the Fiavé site (N-E Italy). *Int. Biodeterior. Biodegrad.* **2013**, *84*, 54–64. [[CrossRef](#)]
30. GB/T 2677.8-1994; Fibrous Raw Material. Determination of Acid-Insoluble Lignin. The State Bureau of Quality and Technical Supervision: Beijing, China, 1994.
31. GB/T 2677.3-1993; Fibrous Raw Material-Determination of Ash. The State Bureau of Quality and Technical Supervision: Beijing, China, 1993.
32. GB-T 1936.1-2009; Method of Testing in Bending Strength of Wood. The State Bureau of Quality and Technical Supervision: Beijing, China, 2009.
33. Cretté, S.A.; Näsänen, L.M.; González-Pereyra, N.G.; Rennison, B. Conservation of waterlogged archaeological corks using supercritical CO<sub>2</sub> and treatment monitoring using structured-light 3D scanning. *J. Supercrit. Fluids* **2013**, *79*, 299–313. [[CrossRef](#)]
34. Brorson, C.B.; Christenson, A. The conservation of waterlogged wood in the National Museum of Denmark. *Stud. Conserv.* **1970**, *15*, 27–44.
35. Guo, J.; Xiao, L.; Han, L.; Wu, H.; Yang, T.; Wu, S.; Yin, Y. Deterioration of the cell wall in waterlogged wooden archeological artifacts, 2400 years old. *IAWA J.* **2019**, *40*, 820–844. [[CrossRef](#)]
36. Hoffmann, P.; Jones, M.A. Structure and Degradation Process for Waterlogged Archaeological Wood. *Archaeol. Wood* **1989**, *225*, 35–65. [[CrossRef](#)]
37. Schwanninger, M.; Rodrigues, J.; Pereira, H.; Hinterstoisser, B. Effects of short-time vibratory ball milling on the shape of FT-IR spectra of wood and cellulose—Science Direct. *Vib. Spectrosc.* **2004**, *36*, 23–40. [[CrossRef](#)]
38. Singh, A.P.; Kim, Y.S.; Chavan, R.R. Relationship of wood cell wall ultrastructure to bacterial degradation of wood. *IAWA J.* **2019**, *40*, 845–870. [[CrossRef](#)]
39. Genestar, C.; Palou, J. SEM–FTIR spectroscopic evaluation of deterioration in an historic coffered ceiling. *Anal. Bioanal. Chem.* **2006**, *384*, 987–993. [[CrossRef](#)] [[PubMed](#)]
40. Pointing, S.; Jones, E.; Jones, A. Decay prevention in waterlogged archaeological wood using gamma irradiation. *Int. Biodeterior. Biodegrad.* **1998**, *42*, 17–24. [[CrossRef](#)]
41. Hoffmann, P. On the long-term visco-elastic behaviour of polyethylene glycol (PEG) impregnated archaeological oak wood. *Holzforschung* **2010**, *64*, 1009010903. [[CrossRef](#)]
42. Fojutowski, A.; Wróblewska, H.; Komorowicz, M.; Kropacz, A.; Noskowiak, A.; Pomian, I. Changes in the properties of English oak wood (*Quercus robur* L.) as a result of remaining submerged in Baltic Sea waters for two years. *Int. Biodeterior. Biodegrad.* **2014**, *86*, 122–128. [[CrossRef](#)]
43. Fojutowski, A.; Wróblewska, H.; Kropacz, A.; Komorowicz, M.; Noskowiak, A.; Pomian, I. Chosen properties of oak wood submerged for 6 months in the Baltic Sea. *Folia For. Pol. Ser. A* **2011**, *42*, 17–30.
44. Komorowicz, M.; Wróblewska, H.; Fojutowski, A.; Kropacz, A.; Noskowiak, A.; Pomian, I. The impact of 5 years' underwater exposure in the Baltic Sea (Puck Bay) on selected properties of English oak wood samples. *Int. Biodeterior. Biodegrad.* **2018**, *131*, 40–50. [[CrossRef](#)]
45. Jordan, B.A. Site characteristics impacting the survival of historic waterlogged wood: A review. *Int. Biodeterior. Biodegrad.* **2001**, *47*, 47–54. [[CrossRef](#)]
46. Kubler, H.; Liang, L.; Chang, L. Thermal Expansion of Moist Wood. *Wood Fiber* **1973**, *5*, 257–267.
47. Kaung, M.; Thanate, R. Coefficient of Thermal Expansion of Rubberwood (*Hevea brasiliensis*) in Convective Drying Process. *J. Trop. For. Sci.* **2020**, *32*, 72–82. [[CrossRef](#)]

48. Espinoza-Herrera, R.; Olmos, L.; Trujillo, I.A.; Garnica-Gonzalez, P. Study of Thermal Expansion and Compression Strength of Three Wood Species from Plantations. *Cerne* **2020**, *26*, 256–264. [[CrossRef](#)]
49. Romagnoli, M.; Galotta, G.; Antonelli, F.; Sidoti, G.; Humar, M.; Kržišnik, D.; Čufar, K.; Petriaggi, B.D. Micro-morphological, physical and thermogravimetric analyses of water-logged archaeological wood from the prehistoric village of Gran Carro (Lake Bolsena-Italy). *J. Cult. Herit.* **2018**, *33*, 33–38. [[CrossRef](#)]
50. Lindfors, E.-L.; Lindström, M.; Iversen, T. Polysaccharide degradation in waterlogged oak wood from the ancient warship Vasa. *Holzforschung* **2008**, *62*, 57–63. [[CrossRef](#)]
51. Pedersen, N.; Jacqueline, L.; Francesca, M.; Charlotte, B. Correlation between bacterial decay and chemical changes in waterlogged archaeological wood analysed by light microscopy and Py-GC/MS. *Holzforschung* **2021**, *75*, 635–645. [[CrossRef](#)]
52. Pizzo, B.; Pecoraro, E.; Sozzi, L.; Salvini, A. Collapsed and re-swollen archaeological wood: Efficiency and effects on the chemical and viscoelastic characteristics of wood. *J. Cult. Herit.* **2021**, *51*, 79–88. [[CrossRef](#)]
53. Swadener, J.; Rho, J.Y.; Pharr, G.M. Effects of anisotropy on elastic moduli measured by nanoindentation in human tibial cortical bone. *J. Biomed. Mater. Res.* **2015**, *57*, 108–112. [[CrossRef](#)]
54. Hori, R.; Wada, M. The Thermal Expansion of Wood Cellulose Crystals. *Cellulose* **2005**, *12*, 479–484. [[CrossRef](#)]
55. Hidaka, H.; Kim, U.-J.; Wada, M. Synchrotron X-ray fiber diffraction study on the thermal expansion behavior of cellulose crystals in tension wood of Japanese poplar in the low-temperature region. *Holzforschung* **2010**, *64*, 167–171. [[CrossRef](#)]